Yonago Acta medica 1996;39:155–162

Three-Dimensional Gd-DTPA Enhanced MR Angiography (MRA): Comparison of the Visualization of Portal Branches by MRA using Magnetization Transfer Contrast Pulses and Fat Saturation Pulse

Yuji Suto, Masayuki Kamba, Takashi Kato, Shuji Sugihara, Kotaro Yoshida and Yoshio Ohta

Department of Radiology, Faculty of Medicine, Tottori University, Yonago 683, Japan

To evaluate the visualization of portal branches of the liver, we compared three-dimensional (3D) gadopentetate dimeglumine (Gd-DTPA) enhanced magnetic resonance angiography (MRA) using magnetization transfer contrast pulses (MTC) with MRA using fat saturation pulse (FAT-SAT). The subjects were 10 healthy volunteers and 15 patients with liver tumors. MRA was reconstructed from the data obtained by 3D-fast low angle shot sequences(FLASH) with MTC after intravenous injection of Gd-DTPA during breath-holding. MRA was performed again on another day by 3D-FLASH with FAT-SAT. The depictabilities of the portal trunk to the 4th-order intrahepatic portal branches of MRA using both methods were compared among healthy volunteers. The depictabilities of the tumor and the contour of the liver were compared in patients with liver tumor. The visualization of the portal trunk was significantly better by the FAT-SAT-MRA. The 1st-order to 2nd-order portal branches were clearly visualized by both MRA sequences, but the depictabilities of the third-order and fourth-order branches were significantly better by the MTC-MRA. The visualization of the contour of the liver was significantly better by the FAT-SAT-MRA, and that of the tumor was significantly better by the MTC-MRA. In conclusion, complementary use of the 2 techniques is recommended in liver MRA.

Key words: magnetization transfer contrast; MR angiography; portal vein

Methods such as two-dimensional (2D)-time-of-flight (TOF) (Edelman et al., 1989a, 1989b; Finn et al., 1991), three-dimensional (3D)-TOF (Lewin et al., 1991; Lewin, 1992; Smith and Bakke, 1993), and 3D-phase contrast angiography (PCA) (Dumoulin et al., 1990; Hausmann et al.,1991; Vock et al., 1991) have been used for abdominal magnetic resonance angiography (MRA), and each method has been suggested to have its own limitations. In 2D-TOF, the visualization of vessels flowing in the slice is reduced, and the image is deteriorated especially in the abdominal region by phase discrepancy due to multiple breath-holding maneuvers (Bosmans et al., 1992; Suto et al., 1994a). In 3D-TOF, signals are reduced due to saturation of blood flow spins in the imaging slab (Lewin, 1992; Bosmans et al., 1992; Suto et al., 1994b). In 3D-PCA, the length of time needed for scanning and image processing was a problem (Suto

Abbreviations: 2D, two-dimensional; 3D, three-dimensional; FA, flip angle; FAT-SAT, fat saturation pulse; FLASH, fast low angle shot sequences; FOV, field of view; Gd-DTPA, gadopentetate dimeglumine; Hf, protons in a free motion state; Hr, protons in a restricted motion state; MIP, maximum intensity projection; Mo, normalized SI obtained without MTC; Mo', normalized SI obtained without FAT-SAT; Mp, mean SI of a phantom obtained with MTC; Mp', mean SI of a phantom obtained with FAT-SAT; MR, magnetic resonance; MRA, MR angiography; MRI, MR imaging; Ms, normalized SI obtained with MTC; Ms', normalized SI obtained with FAT-SAT; MTC, magnetization transfer contrast pulse; PCA, phase contrast angiography; ROI, region of interest; SI, signal intensity; TE, echo time; TOF, time-of-flight; TR, repetition time

et al., 1996). To overcome these problems, MRA utilizing the T1-shortening effect of gadopentetate dimeglumine (Gd-DTPA) (Weinmann et al., 1984; Niendorf et al., 1991) has been evaluated and reported to be useful (Creasy et al., 1990; Prince et al., 1993; Prince, 1994; Suto et al., 1994b, 1996).

We previously reported MRA by bolus intravenous injection of Gd-DTPA and by scanning with a single breath hold (Suto et al., 1994b). This method is free from image deterioration due to phase discrepancy caused by multiple breath holds such as that observed by 2D-TOF; it also allows suppression in the saturation of blood flow spins in the imaging slab such as that observed in 3D-TOF, and can be performed within a short time because it requires only one breath holding period (scanning time about 20 s).

However, the greatest disadvantage of Gd-enhanced MRA is a decrease in the vessel-liver contrast due to contrast enhancement also of the hepatic parenchyma by Gd (Suto et al., 1994b, 1996).

In this study, we added magnetization transfer contrast pulses (MTC) (Wolff and Balban, 1989; Balban and Ceckler, 1992) or fat saturation pulses (FAT-SAT) (Rosen et al., 1984; Frahm et al., 1985) to contrast-enhanced 3D MRA sequences as measures to increase the contrast between vessels and surrounding tissues and compared the usefulness of the 2 methods. These pulses have been used in MRI of the heart (Li et al., 1993), but they have not often been used in breath-holding imaging of the abdominal region, and there have been no comparative studies of MRA using 2 pulses.

Subjects and Methods

Subjects

The subjects were 10 normal male volunteers (aged 30–40 years, mean 36 years) and 15 patients who underwent MRI for liver tumors (aged 30–60 years, mean 48 years). The liver tumors were hepatocellular carcinoma in 6, metastatic liver cancer in 2 (primary lesion located in the colon and pancreas in 1 each), and liver hemangioma in 2. Normal volunteers were examined in advance by ultrasonography and blood biochemical tests, and those who did not have fatty liver were selected. Liver tumor patients who showed no abnormalities on electrocardiography or chest radiography and exhibited mild or no fat infiltration on blood biochemical tests were selected. Prior to the start of each study, informed consent was obtained from each subject.

MTC-MRA

MR imagings were implemented on a 1.5 Tesla whole body MR imaging system using a body phased array coil with 25 mTesla/m maximum gradient amplitude and 1200 μs rise time. The imaging pulses were 3D-fast low angle shot image (FLASH) (Haase et al., 1986) with the addition of 4 MTC [Gaussian waveform, pulse duration 8 ms, interval 5 ms, off-resonance 1.5 kHz, band 250 Hz, radio-frequency (RF) pulse intensity 12.1×10^{-6} Tesla]. The 4 serial MTC correspond to 16 phase encode lines in the slab direction. Centric reordering was made for phase encoding in the slab direction so that the information impressed by RF before data collection would be reflected in the image. The parameters of imaging were as follows: repetition time (TR), 10 ms; echo time (TE), 4 ms; flip angle (FA), 15°; field of view (FOV), 350×350 mm; imaging matrix, 128 (number of phase encodings in the plane) $\times$ 256; slab thickness, 80 mm; 16 partitions; signal averaging, 1; and scanning time 23 s. Using this imaging sequence, oblique coronal shots were obtained with breath holding 75 s after rapid intravenous injection of 0.1 mmol/kg of Gd, and MRA was reconstructed from obtained image data by a maximum-intensity projection (MIP) algorithm (Laub, 1990). A series of projection images were generated with viewing angles of –45° to +45° from the coronal plane at fixed 5° intervals.

FAT-SAT-MRA

The imaging sequence was 3D-FLASH including a single FAT-SAT (Gaussian waveform,

Table 1. Comparison of the visualization of portal branches by FAT-SAT-MRA and MTC-MRA

Vessel†	MTC-MRA	FAT-SAT-MRA	*P* value
Portal vein trunk	4.8 ± 0.2	5.0	*
First-order branches	5.0	5.0	NS
Second-order branches	5.0	5.0	NS
Third-order branches	4.6 ± 0.5	4.2 ± 0.3	**
Fourth-order branches	3.8 ± 0.5	3.0 ± 0.6	**

All values are mean gradings (± SD) for 3 observers.
FAT-SAT-MRA, magnetic resonance angiography obtained with fat saturation pulse; MTC-MRA, magnetic resonance angiography obtained with magnetization transfer contrast pulses; NS, not significant.
†Vessel visualization was graded on a scale of 1 to 5: 1 = vessel not indentified and 5 = vessel clearly defined.
* $P < 0.01$.
** $P < 0.001$.

pulse duration 9.7 ms, off-resonance 250 Hz, band 100 Hz, RF pulse intensity 2.6×10^{-6} Tesla), and one FAT-SAT was adjusted to the 16 phase encode lines in the slab direction. Centric reordering was made similarly to MRA with MTC.

The parameters of imaging were as follows: TR, 10 ms; TE, 4 ms; FA, 15˚; FOV, 350 × 350 mm; imaging matrix,128 (number of phase encodings in the plane) × 256; slab thickness, 80 mm; 16 partitions; signal averaging, 1; and scanning time 19 s. Similar imaging was performed within 1 week after MTC-MRA with image reconstruction by an MIP algorithm.

Analysis of MRA

Evaluation of the effect of MTC

To measure the extent of the effect of MTC in the imaging sequence, 3D-FLASH with and without MTC was performed serially without Gd injection in 10 healthy volunteers, the region of interests (ROIs) were determined in the liver, muscle, perirenal fat layer and portal vein, and the mean signal intensity (SI) per pixel was calculated for each tissue. A phantom filled with a copper sulfate solution was attached to the right flank of each subject, and imaging was made in the area including the phantom. The mean SI of the phantom was expressed as Mp, and the mean SI normalized by dividing SI in each tissue by Mp was expressed as Sln. Sln obtained by the sequence with MTC pulses (Ms) was divided by Sln obtained by the sequence without MTC pulses (Mo), and Ms/Mo was calculated for each tissue.

Evaluation of the effect of FAT-SAT

To evaluate the degree of fat suppression by FAT-SAT, 3D-FLASH with and without FAT-SAT were performed serially before injection of the contrast medium in 10 normal volunteers, ROIs were determined in the liver, muscle, perirenal fat layer and portal vein, and the mean SI per pixel was calculated in each tissue. A phantom filled with copper sulfate solution was attached to the right flank, and imaging was made over the area including the phantom. The mean SI of the phantom was expressed as Mp', and the mean SI normalized by dividing SI by Mp' in each tissue was represented by Sln. Sln obtained by the sequence with FAT-SAT (Ms') was divided by Sln obtained by the sequence without FAT-SAT (Mo'), and Ms'/Mo' was calculated for each tissue.

Comparison of MRAs with MTC and those with FAT-SAT

MRAs obtained by the MIP method were studied in the cine mode. The visibility of the portal trunk from the 1st-order to the 4th-order branches of the portal system was compared between MRA using MTC and MRA using FAT-SAT in 10 normal volunteers. Three uninformed radiologists studied the images individually and assessed the visibility of the

Table 2. Comparison of the visualization of the tumor and the contour of the liver by FAT-SAT-MRA and MTC-MRA

	MTC-MRA	FAT-SAT-MRA	*P* value
Tumor visualization†	3.0 ± 0.3	2.0 ± 0.4	*
Coutour of the liver†	2.8 ± 0.4	4.0 ± 0.5	**

All values are mean gradings (± SD) for 3 observers.
FAT-SAT-MRA, magnetic resonance angiography obtained with fat saturation pulse; MTC-MRA, magnetic resonance angiography obtained with magnetization transfer contrast pulses.
†The visualization of the tumor and the liver contour was graded on a scale of 1 to 4 (1 = poor, 2 = fair, 3 = good, 4 = excellent).
*$P < 0.01$.
**$P < 0.001$.

hepatic vessels according to the following 5-grade scale based on the classification by Goldberg and colleagues (1993): 1, vessel not identified; 2, vessel equivocally identified; 3, vessel identified but poorly defined; 4, vessel identified and moderately well-defined; 5, vessel clearly defined, allowing definite evaluation of patency.

The results of the 2 MRAs were compared by Wilcoxon's signed rank test, and differences were considered significant when the *P* value was less than 0.05. Portal branches were classified according to the Takayasu Classification (Takayasu et al., 1985). Caudal lobe branches were excluded, because they are difficult to anatomically identify.

In the 10 patients with liver tumors, the detectabilities of the tumor and the liver contour were compared between MRAs with MTC and those with FAT-SAT. Evaluation was made

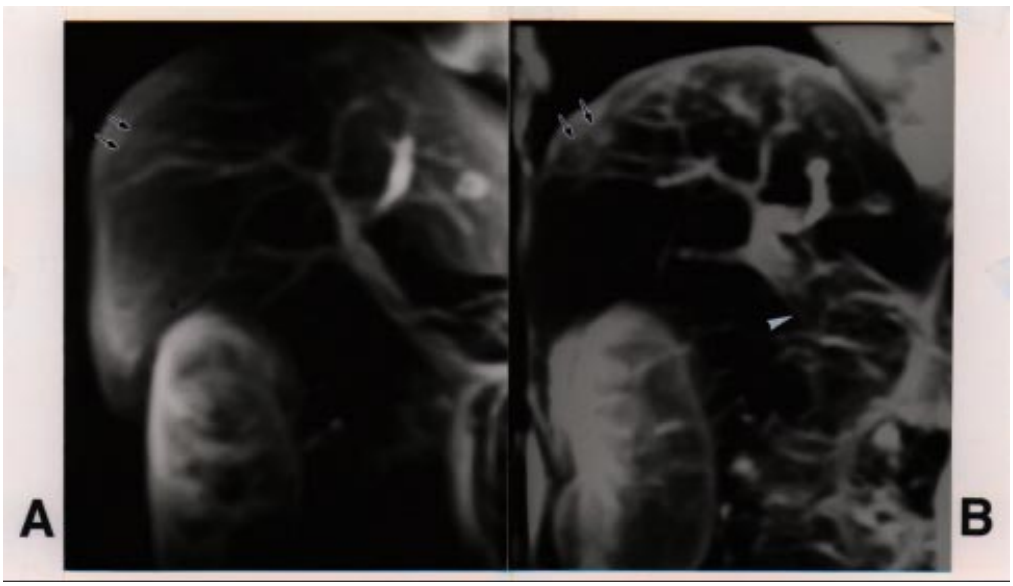

Fig. 1. Case 1 (hepatocellular carcinoma). **A**: magnetic resonance angiography obtained with fat saturation pulse (FAT-SAT-MRA). **B**: magnetic resonance angiography obtained with magnetization transfer contrast pulses (MTC-MRA). The depictabilities of the intrahepatic distal portal branches and the tumor (arrows) are better by MTC- MRA than by FAT-SAT-MRA, except that the visualization of the portal trunk is poor in its caudal portion (arrowhead). The depictabilities of the portal trunk and the contour of the liver are better by FAT-SAT-MRA than by MTC- MRA.

according to the 4-grade scale of: 1, poor (no liver contour or tumor stain is identified); 2, fair (liver contour and tumor stain are identified but equivocal); 3, good (liver contour and tumor stain are identified with moderate clarity); 4, excellent (liver contour and tumor stain can be clearly identified). The findings in the 2 MRAs were compared by Wilcoxon signed rank test, and *P* values less than 0.05 were considered to be significant.

Results

Effects of MTC

The value of Ms/Mo before administration of the contrast material was 0.70 ± 0.07 (mean ± SD) for the liver, 0.98 ± 0.07 for the portal vein, 0.98 ± 0.06 for fat and 0.65 ± 0.08 for muscle. Ms/Mo of the portal vein was near 1, but those of the liver and muscle were low, and MTC was effective in this study.

Effects of FAT-SAT

The value of Ms/Mo before administration of the contrast material was 0.56 ± 0.10 for the liver, 0.52 ± 0.11 for the portal vein, 0.16 ± 0.06 for fat, and 0.22 ± 0.08 for muscle. Ms/Mo of fat was lower than those of other tissues, and the FAT-SAT was effective.

Comparison of MRAs with MTC and those with FAT-SAT

The visualization of the portal trunk was significantly better in FAT-SAT-MRA ($P < 0.01$). The 1st-order and 2nd-order branches of the portal vein were clearly visualized by both MRA sequences, but 3rd-order and 4th-order branches were visualized significantly better by the MTC-MRA ($P < 0.001$). The visualization of the liver contour was significantly better by the FAT-SAT-MRA ($P < 0.001$), and that of the tumor was significantly better by the MTC-MRA ($P < 0.01$) (Tables 1 and 2, Figs.1 and 2).

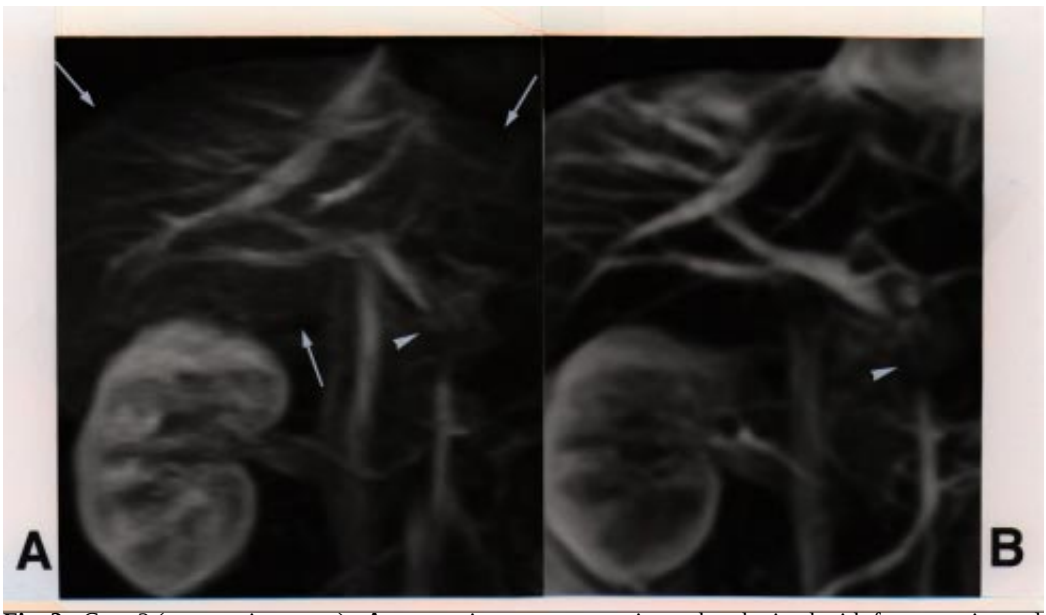

Fig. 2. Case 2 (pancreatic cancer). **A**: magnetic resonance angiography obtained with fat saturation pulse (FAT-SAT-MRA). **B**: magnetic resonance angiography obtained with magnetization transfer contrast pulses (MTC-MRA). The depictabilities of the intrahepatic distal portal branches are better by MTC- MRA than by FAT-SAT-MRA. However, the visualization of the contour (arrows) of the liver is better by FAT-SAT-MRA than by MTC- MRA. Arrowheads: Portal vein obstruction due to tumor invasion.

Discussion

FAT-SAT is a technique to selectively reduce the signals of adipose tissue by impressing selective excitation pulses with a resonance frequency of fat (Rosen et al., 1984; Frahm et al., 1985). In this study, the Ms'/Mo' ratio of fat was reduced below those of other tissues, and signals of the adipose tissue around the liver were reduced. Combined with the enhancement of the SI by the administration of the contrast medium, the contour of the liver tissue was represented more clearly. The portal trunk, which is also surrounded by adipose tissue, was clearly visualized.

MTC is a method to utilize the interaction of magnetization between protons in a free motion state (Hf) and those in a restricted motion state (Hr) (Wolff and Balban, 1989; Balban and Ceckler, 1992) and is useful as a method for contrast enhancement in MRA (Edelman et al., 1992; Pike et al., 1992).

Effects of MTC vary widely depending on the tissue. Since macromolecules are abundantly present in the liver, Hr and Hs are exchanged well. Therefore, MTC are expected to be effective in the liver (Outwater et al., 1992; Loesberg et al., 1993; Kahn et al., 1993; Suto et al., 1996). However, they are hardly effective in adipose tissues not containing Hf (Wolff and Balban, 1989; Balban and Ceckler, 1992). Consequently, MTC makes adipose tissue stand out as a high signal area relative to the liver tissue.

The MIP algorithm is used widely for image processing in MRA (Laub, 1990). By this method, the maximum SI is determined on the pixels of the projected surface. If there are perivascular signals such as those of fat, visualization of vessels is often reduced within MIP images. As mentioned previously, MTC is hardly effective in adipose tissue. While the decrease in the SI due to MTC is minimal in perivascular tissues in the portal trunk surrounded by adipose tissue, the SI is reduced in perivascular adipose tissue by FAT-SAT, resulting in improvements in the visualization of the portal trunk. On the other hand, visualization of the intrahepatic portal system and tumor stain were better by the MTC-MRA than the FAT-SAT-MRA.

There are reports that the SI in the liver is markedly reduced by FAT-SAT in patients who show moderate to severe fat infiltration (Mitchell, 1992). In the subjects of this study, fat infiltration was absent or mild, so that the amount of intrahepatic adipose tissue around the vessel or the tumor is considered to have been smaller than that around the portal trunk. Therefore, the increase in the contrast between the vessel and surrounding liver tissue was small even with impression of FAT-SAT. On the other hand, MTC decreases the SI in liver tissues around the vessels or the tumor, and the SI of the vessels and tumor is increased by the contrast medium, resulting in relative increases in the vessel-liver and tumor-liver contrast.

In contrast, in subjects with marked fat infiltration, the SI of the liver parenchyma is hardly reduced, because MTC has little effect in adipose tissue. In such cases, FAT-SAT-MRA may be more effective. Therefore, MTC-MRA is advantageous for visualization of the distal intrahepatic portal system and the tumor, but FAT-SAT-MRA is advantageous for visualization of the contour of the portal trunk or the liver, which are directly surrounded by adipose tissue, in individuals with mild or no fat infiltration.

Although, concurrent use of both methods is the best, the use of both methods means prolongation of the scanning time with the present system. As a result, imaging with breath-holding becomes impossible, and the inevitable deterioration of the image quality prevents simultaneous application of both techniques to the upper abdominal region. Therefore, complementary use of the 2 techniques is recommended in liver MRA.

References

1 Balban RS, Ceckler TL. Magnetization transfer contrast in MR imaging. Magn Reson Q 1992;8: 116–137.
2 Bosmans H, Marchal G, Hecke PV, Van Hoenacker

P. MRA review. Clin Imaging 1992; 16:152–167.
3 Creasy JL, Price RR, Presbrey T, Goin D,Partain CL, Kessler RM. Gadolinium-enhanced MR angiography. Radiology 1990;175:280–283.
4 Dumoulin C, Yucel, EK, Vock P, Souza SP, Terrier F, Steinberg FL, et al. Two-and three dimensional phase contrast MR angiography. J Comput Assist Tomogr 1990;14:779–784.
5 Edelman RR, Zhao B, Liu C, Wentz KU, Mattle HP, Finn JP, et al. MR angiography and dynamic flow evaluation of the portal venous system. Am J Roentgenol 1989a;153:755–760.
6 Edelman RR, Wentz KU, Mattle HP, Zhao B, Liu C, Kim D, et al. Projection arteriography and venography: initial clinical results with MR. Radiology 1989b;172:351–357.
7 Edelman RR, Ahn SS, Chien D, Li W, Goldmann A, Mantello M, et al. Improved time-of-flight MR angiography of the brain with magnetization transfer contrast. Radiology 1992;184:395–399.
8 Finn JP, Edelman RR, Jenkins RL. Liver transplantation: MR angiography with surgical validation. Radiology 1991;179:265–269.
9 Frahm J, Haase A, Hanicke W, Matthaei D, Bomsdorf H, Helzel T. Chemical shift selective MR imaging using a whole-body magnet. Radiology 1985;156:441–444.
10 Golderberg MA, Yucel EK, Saini S, Hahn P, Kaufman JA, Cohen MS. MR angiography of the portal and hepatic venous systems: preliminary experience with echoplanar imaging. Am J Roentgenol 1993;160:35–40.
11 Haase A, Frahm J, Matthaei D, Merboldt KD, Hanicke W. FLASH imaging: rapid NMR imaging using low flip angle pulses. J Magn Reson 1986;67:258–266.
12 Hausmann R, Lewin JS, Laub G. Phase-contrast MR angiography with reduced acquisition time: new concepts in sequence design. J Magn Reson Imaging 1991;1:415–422.
13 Kahn JCE, Perera SD, Sepponen RE, Tanttu JI, Tierala EK, Lipton MJ. Magnetization transfer imaging of the abdomen at 0.1 T: detection of hepatic neoplasms. Magn Reson Imaging 1993; 11:67–71.
14 Laub G. Displays for MR angiography. Magn Reson Med 1990;14:222–229.
15 Lewin JS. Time-of-flight magnetic resonance angiography of the aorta and renal artery. Invest Radiol 1992;27:84–89.
16 Lewin JS, Laub G, Hausmann R. Three-dimensional time-of-flight MR angiography: application in the abdominal and thorax. Radiology 1991;179:261–264.
17 Li D, Paschal CB, Haacke EM, Adler LP. Coronal arteries: three dimensional MR imaging with fat saturation and magnetization transfer contrast. Radiology 1993;187:401–406.
18 Loesberg AC, Kormano M, Lipton MJ. Magnetization transfer imaging of normal and abnormal liver at 0.1 T. Invest Radiol 1993;28: 726–731.
19 Mitchell DG. Focal manifestations of diffuse liver disease at MR imaging. Radiology 1992; 185:1–11.
20 Niendorf HP, Dinger JC, Haustein J. Tolerance data of Gd-DTPA: a review. Eur J Radiol 1991; 13:15–20.
21 Outwater E, Schnall MD, Braitman LE, Dinsmore BJ, Kressel HY. Magnetization transfer of hepatic lesion: evaluation of a novel contrast technique in the abdomen. Radiology 1992; 182:535–540.
22 Pike GB, Hu BS, Glover GH, Enzmann DR. Magnetization time-of-flight magnetic resonance angiography. Magn Reson Med 1992;25:372–379.
23 Prince MR, Yucel EK, Kaufman JA, Harrison DC, Geller SC. Dynamic gadolinium-enhanced three-dimensional abdominal MR arteriography. J Magn Reson Imaging 1993;3:877–881.
24 Prince MR. Gadolinium-enhanced MR aortography. Radiology 1994;191:151–164.
25 Rosen BR, Wedeen VJ, Brady TJ. Selective saturation NMR imaging. J Comput Assist Tomogr 1984;8:813–818.
26 Smith HJ, Bakke SJ. MR angiography of in situ and transplanted renal arteries: early experience using a three-dimensional time-of-flight technique. Acta Radiol 1993;34:150–155.
27 Suto Y, Kato T, Kimura T, Takizawa O. Use of magnetization transfer contrast to improve single breath-holding three-dimensional MR portography with bolus injection of gadopentetate dimeglumine: a preliminary report. J Magn Reson Imaging 1996;6:295–299.
28 Suto Y, Ohuchi Y, Kimura T, Shirakawa T, Mizuuchi N, Takizawa O, et al. Three-dimensional black blood magnetic resonance angiography of the liver during breath holding: a comparison with two-dimensional time of flight MRA. Acta Radiol 1994a; 35:131–134.
29 Suto Y, Ohuchi Y, Kimura T, Takizawa O, Ohta Y. Single breath-holding three-dimensional magnetic resonance portography with bolus injection of Gd-DTPA in subjects with normal liver: a comparison with two dimensional time of flight technique. Br J Radiol 1994b;67:1078–1082.
30 Takayasu K, Moriyama N, Muramatsu Y, Shima Y, Goto H, Yamada T. Intrahepatic portal vein branches studied by percutaneous transhepatic portography. Radiology 1985;154:31–36.
31 Vock P, Terrier F, Wegmuller H, Mahler F, Gertsch P, Souza SP, et al. Magnetic resonance angiography of abdominal vessels: early experience using the three-dimensional phase-contrast

technique. Br J Radiol 1991; 64:10–16.
32 Weinmann HJ, Laniado M, Muetzel W. Pharmacokinetic of Gd-DTPA/dimeglumine after intravenous injection into healthy volunteer. Physiol Chem Phys Med NMR 1984;16:167–172.
33 Wolff SD, Balaban RS. Magnetization transfer contrast (MTC) and tissue water proton relaxation in vivo. Magn Reson Med 1989;10:135–144.

(Received August 19, Accepted September14, 1996)